Electronic Supporting Information

Ferromagnetically Coupled Dinuclear M^{II} Complexes Based on a Boratriazine Ligand Framework

Jamie M. Savard, [a] *Gabriel Brunet,* [a] *Anandi Srinivasan,*[a] *Muralee Murugesu,**[a] *and Jaclyn L. Brusso**[a]

[a] Department of Chemistry and Biomolecular Sciences, University of Ottawa, Ottawa, Ontario K1N6N5, Canada.

Contents (9 pages)

General Procedures: The reagents NaN_3, obtained from Acros Organics, anhydrous $FeCl_2$ and $CoCl_2$, obtained from Alfa Aesar, were used as received. Anhydrous solvents (acetonitrile, methanol and diethyl ether) were of reagent grade. The ligand 2,2-difluoro-4,6-bis(2-pyridyl)-1,3-dihydro-1,3,5,2-triazaborinine (Py_2F_2BTA) was synthesized according to literature procedures.[1] IR spectra of solid samples were recorded on an Agilent Technologies Cary 630 FT-IR spectrometer.

Synthesis of $[Fe_2^{II}(\mu_{1,1}\text{-}N_3)_2(N_3)_2(Py_2F_2BTA)_2]$ (22): $FeCl_2$ (14 mg, 0.11 mmol) and NaN_3 (18 mg, 0.28 mmol) were dissolved and stirred in methanol (10 mL) then combined with Py_2F_2BTA (30 mg, 0.11 mmol) dissolved in acetonitrile (10 mL) to afford an opaque, green solution that was then stored at RT. After 48 hours, crystallization was completed, and black blocks were separated from the solution then washed with acetonitrile and diethyl ether. Yield = 78%, IR ϑ_{max} = 3108 (br), 3060 (br), 2965 (br), 2059 (s), 1633 (s), 1598 (m), 1571 (w), 1492 (s), 1467 (s), 1425 (s), 1331 (m), 1284 (s), 1269 (m), 1212 (w), 1190 (w), 1158 (w), 1131 (m) , 1161 (w), 1107 (w), 1081 (m), 1049 (w), 1036 (m), 1015 (m), 992 (w), 972 (s), 898 (w), 846 (m), 815 (m), 788 (w), 745 (s), 713 (s).

Synthesis of $[Co_2^{II}(\mu_{1,1}\text{-}N_3)_2(N_3)_2(Py_2F_2BTA)_2]$ (23): The synthetic procedure followed is the same as that mentioned above using $CoCl_2$ (14 mg, 0.11 mmol), NaN_3 (18 mg, 0.28 mmol), methanol (15 mL), Py_2F_2BTA (30 mg, 0.11 mmol), and acetonitrile (15 mL). After 24 hours, crystallization was completed, and orange blocks were separated from the solution then washed with acetonitrile and diethyl ether. Yield = 85%, IR ϑ_{max} = 3060 (br), 2943 (br), 2833 (br), 2060 (s), 2050 (s), 1635 (s), 1599 (m), 1572 (w), 1496 (s), 1465 (s), 1427 (s), 1376 (w), 1334 (m), 1287 (s), 1267 (s), 1158 (w), 1129 (m), 1107 (m), 1083 (m), 1027 (s), 1016 (s), 993 (m), 973 (s), 899 (w), 850 (m), 814 (m), 746 (s), 714 (s), 670 (m).

Crystallography: Crystallographic data as well as data collection and refinement of complex **1** and complex **2** are summarized in Table **S1**. Selected bond distances and bond angles are given in Table **S2**. The crystals were mounted on thin glass fibers using super glue. Prior to data collection crystals were cooled to 200(2) K. Data were collected on a Bruker AXS KAPPA single crystal diffractometer equipped with a sealed Mo tube source (wavelength 0.71073 Å) APEX II CCD detector. Raw data collection and processing were performed with APEX II software package from Bruker AXS. Systematic absences in the diffraction data and unit-cell parameters were consistent with monoclinic $P2_1/c$ (No.14) for complexes **1** and **2**. Solutions in the centrosymmetric space groups for complexes **1** and **2** yielded chemically reasonable and computationally stable results of refinement. The structures were solved by direct methods, completed with differential Fourier transformation, and refined with full-matrix least-squares procedures based on F^2. Refinement results for complexes **1** and **2** both suggested several non-merohedrally twinned domains. Careful examination of the original data frames and precession images for each complex confirmed the initial twinning assumption. In order to find the independent orientation matrices 307 reflections were collected for **1** and 604 reflections were collected for **2** in different sections of the Ewald sphere. The collected reflection data were then processed with CELL_NOW software[2] and two independent orientation matrices were obtained. Data sets were re-integrated with two independent matrices and treated for twinning absorption corrections and consecutive model refinement was preformed using HKL5 formatted reflection data file. Twining domain ratio coefficients (BASF) for complex **1** and **2** were allowed to refine freely and converged at a ratio of 0.504(1):0.496(1) and 0.511(2):0.489(2) for **1** and **2** respectively. For both complexes all non-hydrogen atoms were refined with anisotropic thermal motion approximation. All hydrogen atom positions were calculated based on the geometry of related non-hydrogen atoms, except for the N-H groups that were located using the Fourier difference maps and refined freely.

Table S1. Crystal data and structure refinement details for complexes **1** and **2**.

	1	**2**
Empirical formula	$C_{24}H_2B_2F_4Fe_2N_{22}$	$C_{24}H_2B_2F_4Co_2N_{22}$
Formula weight	825.94	832.10
Crystal system	Monoclinic	Monoclinic
Space group	$P2_1/c$	$P2_1/c$
Temperature, K	200(2)	200(2)
Calculated density, g/cm^3	1.672	1.714
a, Å	11.9622(3)	11.8492(2)
b, Å	10.2305(2)	10.2697(1)
c, Å	14.0273(3)	13.9894(2)
α, °	90	90
β, °	107.128(1)	107.402(2)
γ, °	90	90
V, Å^3	1640.52(6)	1624.4(4)
Z	2	2
Final R indices [I>2σ(I)]	R_1 = 0.0563; wR_2 = 0.1185	R_1 = 0.0454; wR_2 = 0.1076

Table S2. Selected bond lengths (Å) for complexes **1** and **2**.

Distance (Å)	**1**	**2**
M1–N1	2.191(3)	2.166(5)
M1–N2	2.120(2)	2.074(4)
M1–N3	2.195(3)	2.170(5)
M1–N6	2.063(3)	2.060(4)
M1–N6(a)	2.240(3)	2.163(4)
M1–N9	2.168(2)	2.155(4)
M1–M1(a)	3.3461(7)	3.280(1)

Table S3. Potential short contacts (Å) and angles (°) in complexes **1** and **2**.

1				**2**			
D–H···A	d(D–H)	d(H···A)	<(DHA)	D–H···A	d(D–H)	d(H···A)	<(DHA)
N4–H···N11	0.84(3)	2.09(4)	160	N4–H···N11	0.92(6)	2.01(6)	161
N5–H···N11	0.84(2)	2.05(3)	165	N5–H···N11	0.95(8)	1.91(8)	175
C3–H···F2	0.95	2.54	140	C3–H···F2	0.95	2.53	139
C4–H···N11	0.95	2.54	163	C4–H···N11	0.95	2.53	164
C9–H···N11	0.95	2.49	163	C9–H···N11	0.95	2.53	162
d(F1···N3C8C9C10C11C12 centroid) 3.169(3)				d(F1···N1C1C2C3C4C5 centroid) 3.003(4)			

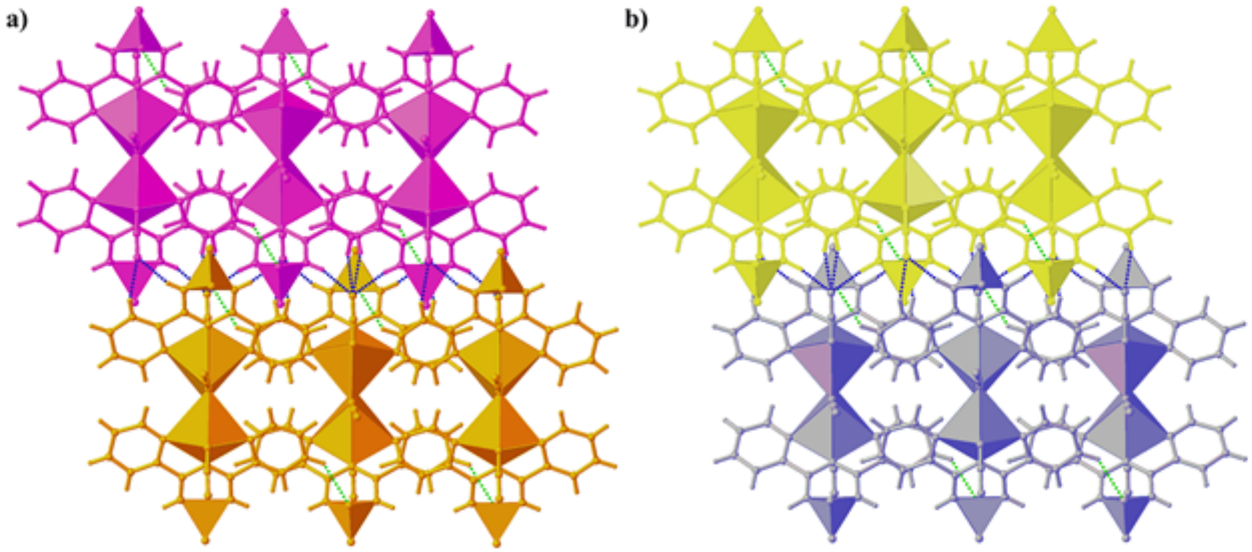

Figure S1. Crystal packing diagram of complex a) **1** and b) **2**. Hydrogen bonds are denoted as green (F···H–A) and blue (N···H–A) dotted lines. Polyhedra added to show orientation of units.

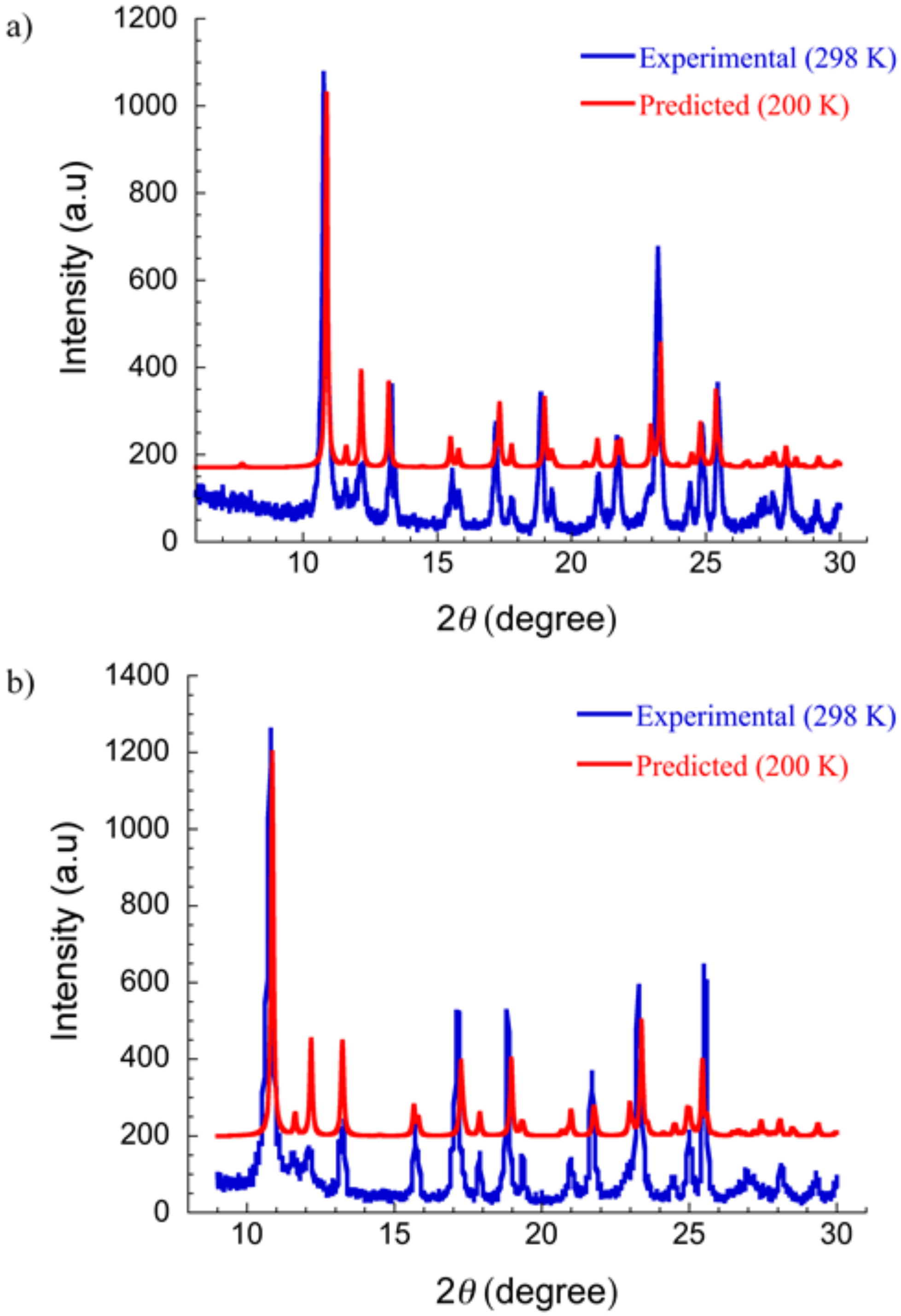

Figure S2. PXRD pattern overlay of experimental microcrystalline samples of a) **1** and b) **2** with their predicted patterns (using the Mercury software).

Table S4. Results from Shape analysis.

	HP-6	**PPY-6**	**OC-6**	**TBR-6**	**JPPY-6**
Complex 1	34.28367	21.45262	2.79146	11.10531	25.46030
Complex 2	34.35301	21.33829	2.66626	11.02944	25.39810

HP-6: Hexagon (D_{6h}); PPY-6: Pentagonal pyramid (C_{5v}); OC-6: Octahedron (O_h); TPR-6: Trigonal prism (D_{3h}); JPPY-6: Johnson pentagonal pyramid (C_{5v})

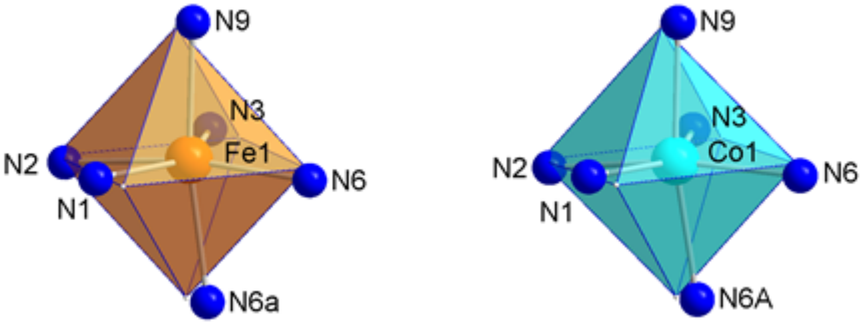

Figure S3. Deviation from ideal octahedral environment about the metal ion in complexes **1** and **2.**

Magnetic Measurements

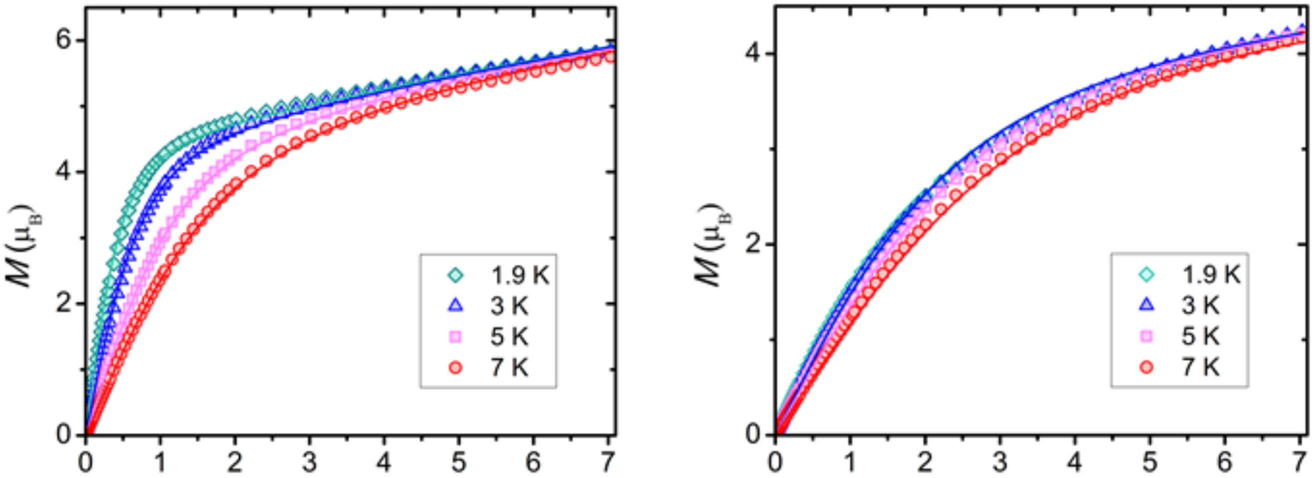

Figure S4. *M vs H* plots for complex **1** (*left*) and **2** (*right*), between 1.9 and 7 K. The solid lines correspond to the best fit obtained using the model described in the main text.

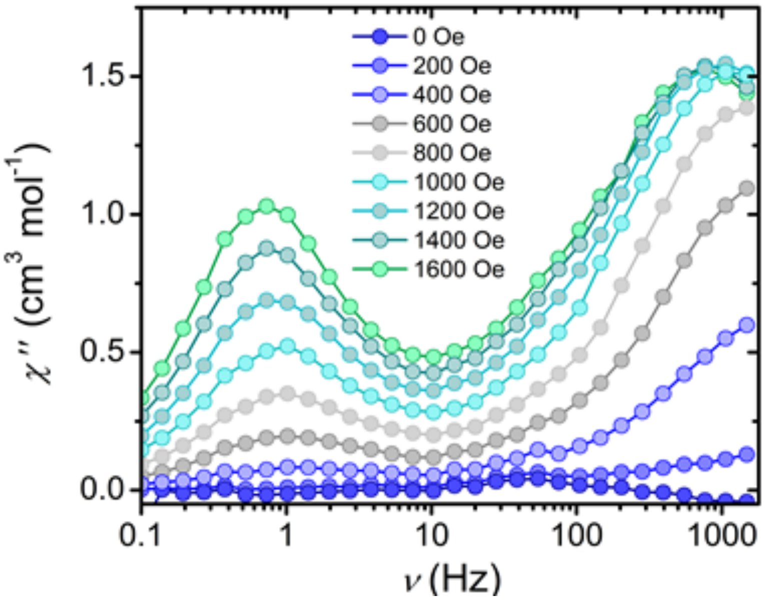

Figure S5. Frequency dependence of the out-of-phase (χ'') magnetic susceptibility for complex **1** collected at 1.9 K and varying dc fields. Solid lines are guides for the eyes.

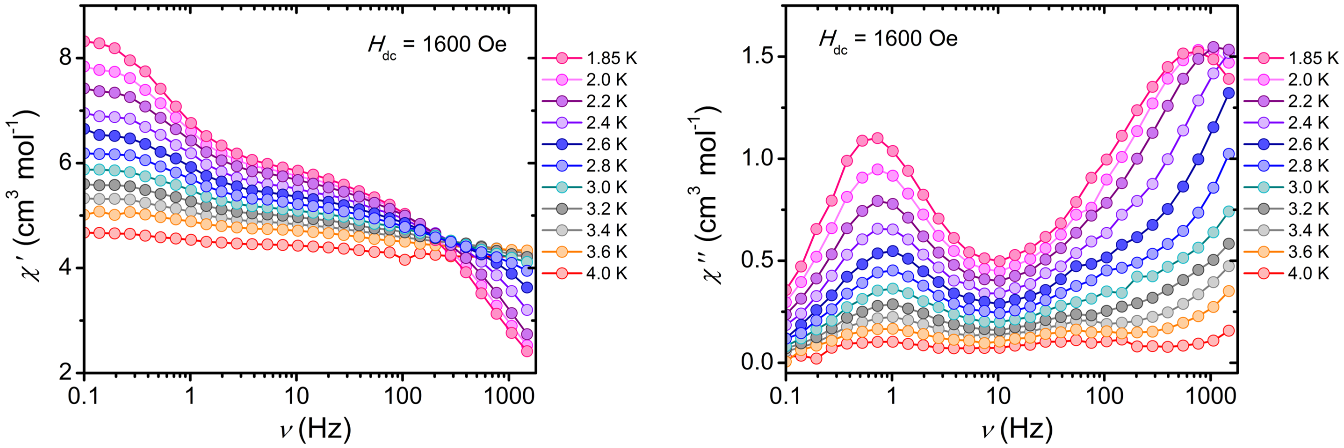

Figure S6. Frequency dependence of the in-phase (χ') and out-of-phase (χ'') magnetic susceptibilities for **1**, collected under a 1600 Oe dc field and varying temperatures. Solid lines are guides for the eyes.

Table S5. Dinuclear Co^{II} and Fe$^{III/II}$ complexes bridged by double EO azido groups.

Compounds	**M–N–M (°)**	**M–M' distance (Å)**	**Coupling constant J (cm^{-1})**	**Ref.**
$[Co_2\,(\mu_{1,1}\text{-}N_3)_2(Py_2F_2BTA)_2(N_3)_2]$	102.0	3.280(1)	7.1(9)	This work
$[Co_2(immepy)_2(N_3)_4]\cdot 2EtOH$	103.40	3.344(6)	17.70^{a}	3
$[Co_2(DMphen)_2(N_3)_4]$	104.9	3.325(2)	14.3(3)	4
$[Co_2(8\text{-}qoac)_2(N_3)_2(H_2O)_2]$	99.22	3.2262(7)	10.4^{a}	5
$[Co_2(biq)_2(\mu_{1,1}\text{-}N_3)_2(N_3)_2]$	104.9, 104.4	3.304(2), 3.276(3)	12.1(2)	6
$[Co_2(biq)_2(\mu_{1,1}\text{-}N_3)_2Cl_2]$	104.1	3.243(2)	13.8(1)	6
$[Co_2(dmbpy)_2(\mu_{1,1}\text{-}N_3)_2(N_3)_2]$	104.1	3.271(1)	13.1(1)	6
$[Co_2(N_3)_2L^2(ClO_4)_2]\cdot 2MeCN$	104.8	3.276(2)	6.0^{a}	7
$[Co_2(DMP)_2(N_3)_4]$	102.29	3.2930(4)	18.1^{a}	8
$[Co_2(PymPz)_2(N_3)_4]$	102.38	3.2470(6)	10.45^{a}	9
$[Co_2(dmphen)_2(\mu_{1,1}\text{-}N_3)_2Cl_2]$	104.86	3.2733(2)	12.0(7)	10
$[Co_2(TDTA)Co(\mu_{1,1}\text{-}N_3)_2(TDTA)]\cdot(ClO_4)_2$	97.99	3.1685(9)	8.5^{a}	11
$[Fe_2^{II}(\mu_{1,1}\text{-}N_3)_2(Py_2F_2BTA)_2(N_3)_2]$	102.0	3.3461(7)	5.7(9)	This work
$[Fe_2^{III}L_2(\mu_{1,1}\text{-}N_3)_2(N_3)_2]$	107.79	3.4134(8)	1.08(1)	12
$[Fe^{III}(salpn)N_3]$	107.1	3.408(1)	0.76^{a}	13

^{a}*Coupling constant reported in the literature without esd's*

References

1. M. Yousaf, N. J. Yutronkie, R. Castañeda, J. A. Klein and J. Brusso, *New J. Chem.*, 2017, **41**, 12218.
2. G. M. Sheldrick, Cell_Now, Bruker-AXS. Madison, WI, **2004**.
3. L. Wang, B. Zhao, C. Zhang, D. Liao, Z. Jiang and S. Yan, *Inorg. Chem.,* 2003, **42**, 5804.
4. T. Liu, D. Fu, S. Gao, Y. Zhang, H. Sun and G. Su, *J. Am. Chem. Soc.,* 2003, 1**25**, 46, 13976.
5. X. N. Cheng, W. X. Zhang and X. M. Chen, *J. Am. Chem. Soc.*, 2007, **129**, 51, 15738.
6. H. Z. Kou, S. Hishiya and O. Sato, *Inorganica Chim. Acta*, 2008, **361**, 2396.
7. M. G. B. Drew, C. J. Harding and J. Nelson, *Inorganica Chim. Acta*, 1996, **246**, 73.
8. S. Q. Bai, E. Q. Gao, Z. He, C. J. Fang and C. H. Yan, *New J. Chem.*, 2005, **29**, 935.
9. A. Jana, S. Konar, K. Das, S. Ray, J. A. Golen, A. L. Rheingold, L. M. Carrella, E. Rentschler, T. Kumar and S. Kumar, *Polyhedron*, 2012, **38**, 258.
10. J. Yuan, W. B. Shi and H. Z. Kou, *Transit. Met. Chem.*, 2015, **40**, 807.
11. M. G. Sommer, R. Marx, D. Schweinfurth, Y. Rechkemmer, P. Neugebauer, M. Van Der Meer, S. Hohloch, S. Demeshko, F. Meyer, J. Van Slageren and B. Sarkar, *Inorg. Chem.*, 2017, **56**, 1, 402.
12. S. Naiya, M. G. B. Drew, C. Diaz, J. Ribas and A. Ghosh, *Eur. J. Inorg. Chem.*, 2011, 4993.
13. K. R. Reddy, M. V. Rajasekharan and J.P. Tuchagues, *Inorg. Chem.*, 1998, **37**, 5978.